17th World Conference on Earthquake Engineering, 17WCEE
Sendai, Japan - September 13th to 18th 2020

SEISMIC RESPONSE ANALYSES OF STEEL MOMENT-RESISTING FRAMES DURING COLLAPSE UNDER SEVERE EARTHQUAKE

S. Mukaide [1], D. Matsukawa [2], R. Sato [3]

[1] *Associate Professor, Osaka Institute of Technology, seiji.mukaide@oit.ac.jp*
[2] *Graduate Student, Osaka Institute of Technology, m1m18212@st.oit.jp*
[3] *Graduate Student, Osaka Institute of Technology, m1m19210@st.oit.jp*

Abstract

Buildings may completely collapse when subjected to ground motion that exceeds their design level. In a previous study, a full-scale four-story steel building was tested at the E-Defense three-dimensional shaking table facility in Japan to evaluate the structural and functional performance of a steel moment-resisting frame under severe earthquake conditions. The collapse of the specimen was characterized by deteriorating behavior caused by the local buckling of columns on the first story. In another study, the authors proposed a precise and simple analytical model for steel moment-resisting frames, where multi-spring models that consider strength deterioration due to local buckling are employed for rectangular hollow section columns. Considering the above background, this study investigates the collapse behavior of steel moment-resisting frames with various column specifications using the simple analytical model.

Parametric analyses are conducted with three-dimensional models that consider the strength deterioration of beams and columns. The analyzed frames are based on the E-Defense specimen, which consisted of beams with wide-flange sections, columns with square hollow sections, concrete slabs with deck plates, and column bases with anchor bolts. The thickness and steel class of the columns are adopted as parameters. The columns are designed so that their bending strength is higher than that of the beams. Half-cycle sine waves in various directions and four recorded seismic motions are employed as input ground motions.

The analysis results are as follows. For each case, the total-collapse mechanism initially occurs. Then, in the cases with frames with thicker columns, all of the stories collapse completely via the same mechanism. In the cases with frames with thinner columns, the collapse mechanism changes from the total-collapse type to the story-collapse type due to strength deterioration. This tendency is the same as that in previously published two-dimensional analyses. To evaluate the collapse resistance capacity, the velocity conversion value of the damage-causing earthquake input energy in arbitrary lateral directions $V_{dm4}(\phi)$ is employed. The values of $V_{dm4}(\phi)$ in the diagonal direction tend to be higher than those in the straight diagonal direction for frames that exhibit the total-collapse mechanism. The opposite trend is observed for frames that exhibit the story-collapse mechanism. The maximum values of $V_{dm4}(\phi)$ for the recorded seismic motions are in good agreement with those for the half-cycle sine waves in various directions.

Keywords: time history analysis, extremely nonlinear behavior, strength degradation, collapse resistance capacity

1. Introduction

Buildings may collapse when subjected to ground motion that exceeds their design level. Exceedingly large ground motions sometimes cause severe damage (for example, the 1995 Kobe earthquake). In a previous study, a full-scale four-story steel building was tested on a shaking table at the E-Defense three-dimensional shaking table facility in Japan [1, 2] to evaluate the structural and functional performance of a steel frame under severe earthquake conditions. The collapse of this building was characterized by deteriorating behavior caused by the local buckling of columns on the first story. To simulate the behavior of local buckling, a collaborative structural analysis system with finite element analysis was proposed [3]. The high-accuracy analysis obtained with this system can reproduce the collapse behavior observed in the shaking table test. However, this analysis is very complicated and thus has a high computational load. In another study, the authors proposed a precise and simple analytical model for steel moment-resisting frames [4], where multi-spring models that consider strength deterioration due to local buckling are employed for rectangular hollow section columns. Considering the above background, the present study investigates the collapse behavior of steel moment-resisting frames with various column specifications using the simplified analytical model.

2. Analysis Plan

2.1 Analysis objects

The original frame [1] was the four-story steel moment-resisting frame shown in Fig. 1. The frame was designed to conform to the Japanese Building Standard Law. The building plan was 10 m in the longitudinal Y direction and 6 m in the transverse X direction. Each story was 3.5 m high, making the overall building height equal to 14 m. The specimen consisted of columns with rectangular hollow sections, beams with wide-flange sections, concrete slabs with deck plates, and column bases with anchor bolts. The original frame was made of one material and used the same sections for all columns. The parameters in the present study are the column specifications listed in Table 1. The parameters include the manufacturing process, steel grade, and width-to-thickness ratio D_c/t_c. The external dimension D_c is 300 mm for all columns. All the columns of each frame have the same values for these parameters. Nine frames were analyzed. The beam sections and material properties are shown Tables 2 and 3, respectively.

Table 1 – Parameters of frames

Frame	Column material (steel grade, manufacturing process)	D_c/t_c (D_c = column width, t_c = column thickness)
BBt9	490 N/mm^2 class, built-up box	33 (D_c = 300 mm, t_c = 9 mm)
BBt12		25 (D_c = 300 mm, t_c = 12 mm)
BBt16		19 (D_c = 300 mm, t_c = 16 mm)
BPt9	490 N/mm^2 class, cold-press-formed	33 (D_c = 300 mm, t_c = 9 mm)
BPt12		25 (D_c = 300 mm, t_c = 12 mm)
BPt16		19 (D_c = 300 mm, t_c = 16 mm)
BRt9	400 N/mm^2 class, cold-roll-formed	33 (D_c = 300 mm, t_c = 9 mm)
BRt12		25 (D_c = 300 mm, t_c = 12 mm)
BRt16		19 (D_c = 300 mm, t_c = 16 mm)

Table 2 – List of beam sections

Floor	G1	G11	G12
R	H-346×174×6×9	H-346×174×6×9	H-346×174×6×9
4	H-350×175×7×11	H-350×175×7×11	H-340×175×9×14
3	H-396×199×7×11	H-400×200×8×13	H-400×200×8×13
2	H-400×200×8×13	H-400×200×8×13	H-390×200×10×16

Wide flange: height × width × web thickness × flange thickness (units: mm)

Table 3 – Material properties

Member		Young's modulus, E (kN/mm^2)	Yield stress, σ_y (N/mm^2)	Tensile strength, σ_u (N/mm^2)
Column	490 N/mm^2 class, built-up box 490 N/mm^2 class, cold-press-formed	205	357.5	490
	400 N/mm^2 class, cold-roll-formed	205	324.5	400
Beam		205	235	400

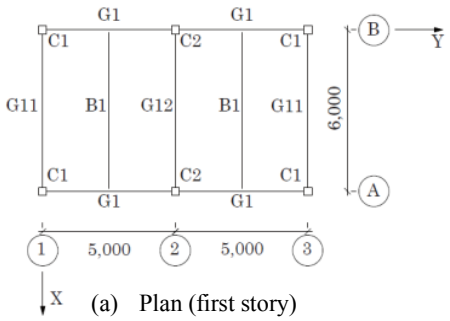

(a) Plan (first story)

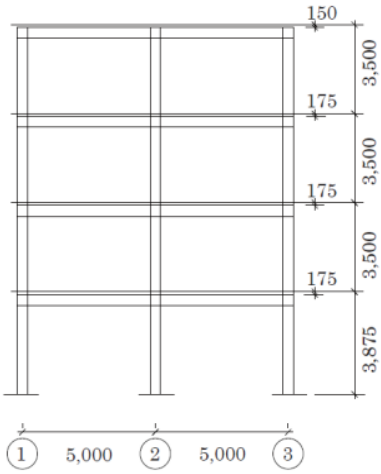

(b) Y-elevation

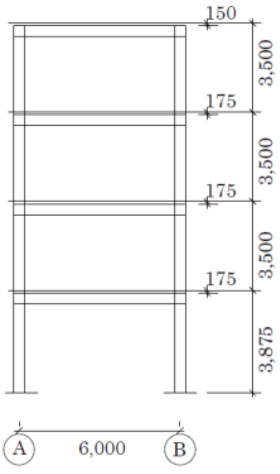

(c) X-elevation

(Units: mm)

Fig. 1 – Framing plan and elevation of specimen

2.2 Analysis model

Fig. 2 shows a schematic diagram of the three-dimensional frame structure model for seismic response analysis. A multi-spring model that covers the range of deterioration due to local buckling was employed for the plastic zone of the column end. The restoring force characteristics of the compression side can be represented by penta-linear segments, as shown in Fig. 3 [4]. The parameters used for determining the curve are listed in Table 4. This is an improved model based on previous studies [5-7]. The restoring force characteristics of the tensile side can be represented by a tri-linear model determined by the yield stress, tensile stress, and stiffness. The secondary stiffness of a material with a low yield ratio (built-up box and cold-press-formed) is 0.01E, and that of a material with a high yield ratio (cold-roll-formed) is 0.005E. The tertiary stiffness is 0.001E. The Meng-Ohi hysteretic rule [8] was employed ($\varphi = 0.5$, $\psi = 5$). A simple plastic hinge was used for analyzing composite beams that consisted of a steel beam and a concrete slab. The restoring force characteristics for the sagging moment were taken from a perfect elastic-plastic model. A Kato-Akiyama skeleton curve, which covered the range of deterioration, was employed for the restoring force characteristics for the hogging moment. The Meng-Ohi hysteretic rule [8] was employed for composite beams ($\varphi = 0.5$, $\psi = 5$). A simple plastic hinge was used for analyzing beam-to-column panels. The restoring force characteristics of the panels were bi-linear and accounted for shear deformation. As described above, for columns and beams, a model that takes into account the strength deterioration due to local buckling was adopted.

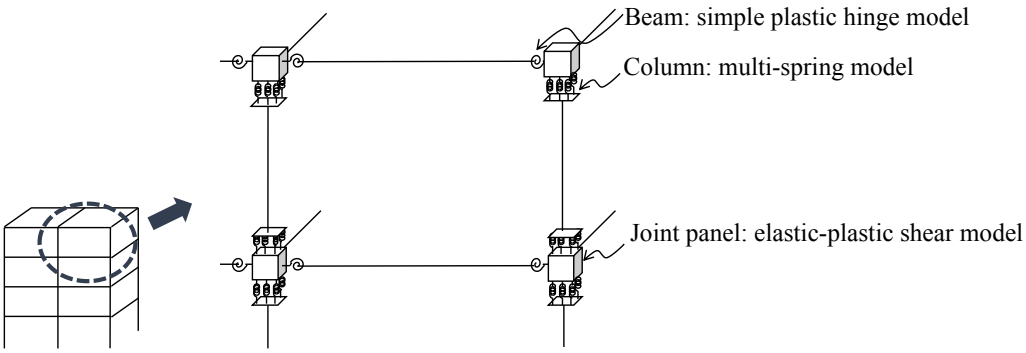

Fig. 2 – Schematic diagram of the three-dimensional frame structural model

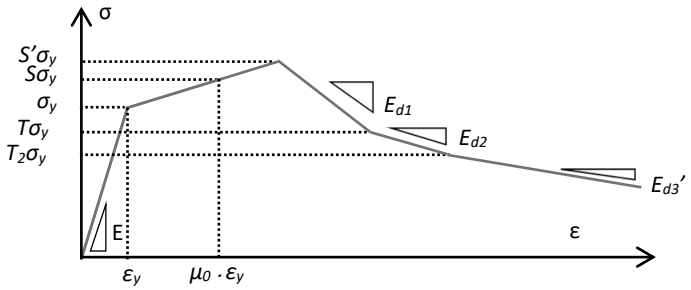

Fig. 3 – Restoring force characteristics for columns on compression side

Table 4 – Parameters used for determining restoring force characteristics of compression side

	Built-up box	Cold-press-formed	Cold-roll-formed
Plastically deformed region, $L_B = 0.8L_s$	$L_S = D$ ($14.3 \leqq D/t \leqq 50$)	$L_S = D$ ($16 \leqq D/t \leqq 50$)	$L_S = D$ ($26 \leqq D/t \leqq 54.7$) $L_S = 0.17+0.032D/t$ ($26 \leqq D/t \leqq 54.7$)
Plasticity rate, μ_0	$\mu_0 = 16.0/\alpha$-12.7 ($3.01 \leqq 1/\alpha \leqq 1.09$) $\mu_0 = 4.8/\alpha$-0.52 ($1.09 \leqq 1/\alpha \leqq 0.23$)	$\mu_0 = 17.4/\alpha$-9.6 ($2.51 \leqq 1/\alpha \leqq 0.72$) $\mu_0 = 4.8/\alpha$-0.52 ($0.72 \leqq 1/\alpha \leqq 0.23$)	$\mu_0 = 8.7/\alpha$-1.20 ($2.62 \leqq 1/\alpha \leqq 0.19$)
First degradation gradient, E_{d1}	$E_{d1}/E = -0.014\,\alpha^2$-0.005		
Second degradation gradient, E_{d2}	$E_{d2}/E = -0.005$ ($3.70 \leqq \alpha \leqq 0.62$)		
Third degradation gradient, E_{d3}	$E_{d3}/E = -0.001$		
Stress rise rate, S'	$S' = 1.2\,S$		$S' = 1.1\,S$
S	$1/S = 0.710+0.167\alpha$		$1/S = 0.778+0.13\alpha$
T/S	$T/S = -0.079\,\alpha+0.81$ ($3.70 \leqq \alpha \leqq 0.62$)		
T_2/T	$T_2/T = 0.90$		

2.3 Analysis conditions

The frames were analyzed using the program SNAP Ver.7 (Kozosystem Group), which considers geometric non-linearities. The program uses the Newmark time integration method ($\beta = 0.25$). Rayleigh damping was considered. A damping ratio of 2% was assigned to the first and second vibration modes.

Four earthquakes, shown in Table 5, were employed in the incremental dynamic analysis. They were scaled by increasing the peak ground velocity (PGV) by 0.1 m/s such that the frame collapsed completely. Here, complete collapse means that story shear forces degrade to zero for some stories under consideration of the P-Δ effect. The analytical results (shown later) are based on the condition with the lowest PGV that led to complete collapse. It is known that the input of two horizontal components and the input of three components, including UD components, show almost the same collapse behavior as that for an earthquake input [9].

In addition to seismic waves, sine waves were used as input motions to evaluate the seismic energy capacities of the frames. The energy absorption performance of frames has been previously evaluated by inputting a half-cycle sine wave in an arbitrary horizontal direction [10]. Therefore, in the present analysis, half-cycle sine waves in various horizontal directions (0°, 15°, 30°, 45°, 60°, 75°, and 90°) were employed. Here, the X and Y directions correspond to 0° and 90°, respectively. The acceleration A of a half-cycle sine wave is derived as:

$$A = \begin{cases} \pi \dfrac{PGV}{T_1} \sin\left(2\pi \dfrac{t}{T_1}\right) & \left(0 \leq t < \dfrac{T_1}{2}\right) \\ 0 & \left(\dfrac{T_1}{2} \leq t\right) \end{cases} \quad (1)$$

where T_1 is the first natural period and t is time.

Table 5 – Input conditions

	Direction	Component	PGA (m/s)	PGV (m/s)
El Centro 1940	Y	NS	4.63	0.45
	X	EW	2.85	0.50
Hachinohe 1952	Y	NS	3.04	0.46
	X	EW	2.38	0.50
Taft 1968	Y	EW	4.97	0.50
	X	NS	4.31	0.44
Takatori 1995	Y	NS	8.57	1.28
	X	EW	8.49	1.28

3. Results and Discussion

3.1 Collapse mechanism

The mechanism at the time of complete collapse is considered. Table 6 lists the number of collapsed stories when a half-cycle sine wave was input. For most cases with frames with t_c = 16 mm, the total-collapse mechanism occurs; all stories collapse completely via the same mechanism. For most cases with frames with t_c = 9 and 12 mm, the total-collapse mechanism initially occurs but then changes to the story-collapse type due to strength deterioration. The inflection point is moved due to strength degradation, and thus the moment at the column ends becomes larger than that for the total-collapse mechanism. Therefore, the mid-story columns become plastic even though the column-to-beam strength ratio is higher than 1.0. In addition, when the input angle is oblique, the number of collapsed stories decreases because the apparent column-to-beam strength ratio decreases due to the biaxial bending of the column. As above, the number of collapsed stories increases as the column-to-beam strength ratio increases, as in the case of a plane frame [11], even for three-dimensional frames with different column design conditions.

Table 6 – Collapsed stories for half-cycle sine waves

	0°	15°	30°	45°	60°	75°	90°
BBt9 frame	1-2	1	1	1	1	1	1-2
BBt12 frame	1-4	1-4	1-2	1-2	1-2	1-2	1-2
BBt16 frame	1-4	1-4	1-4	1-4	1-4	1-4	1-4
BPt9 frame	1-2	1	1	1	1	1	1-2
BPt12 frame	1-4	1-4	1-2	1-2	1-2	1-2	1-2
BPt16 frame	1-4	1-4	1-4	1-4	1-4	1-4	1-4
BRt9 frame	1-2	1	1	1	1	1	1-2
BRt12 frame	1-2	1-2	1-2	1-2	1-2	1-2	1-2
BRt16 frame	1-4	1-4	1-4	1-2	1-2	1-4	1-4

Hyphenated numbers indicate the range of fully collapsed stories.

3.2 Seismic energy capacity

The seismic energy capacity in an arbitrary horizontal direction is considered. A velocity conversion value of the damage-causing earthquake input energy in arbitrary directions $V_{dm4}(\phi)$ was employed. The maximum value of $V_{dm4}(\phi)$ has been proposed as an index for seismic energy capacity [9]. The story shear in arbitrary directions at the i-th story $Q_i(\phi)$ and the inter-story deformation $\delta_i(\phi)$ are calculated as:

$$Q_i(\phi) = Q_{xi}\cos\phi + Q_{yi}\sin\phi \tag{2}$$

$$\delta_i(\phi) = \delta_{xi}\cos\phi + \delta_{yi}\sin\phi \tag{3}$$

where Q_{Xi} and Q_{Yi} are the story shear forces in the X and Y directions, respectively, on the i-th story and δ_{Xi} and δ_{Yi} are the inter-story deformations in the X and Y directions, respectively, on the i-th story. In addition, ϕ was set from 0° to 180° when $Q_i(\phi)$ was greater than or equal to 0, and ϕ was set from 180° to 360° when $Q_i(\phi)$ was less than 0. The damage-causing earthquake input energy in arbitrary directions $E_{dm4}(\phi)$ is calculated as:

$$E_{dm4}(\phi) = \left\{ \sum_{i=1}^{N} \int Q_i(\phi) \bullet d\delta_i(\phi) \right\}_{\max} \tag{4}$$

where N is the number of stories (here, $N = 4$). $E_{dm4}(\phi)$ is a component that separates the total energy into energies in four orthogonal directions. The velocity conversion value of the energy that contributes to damage in arbitrary directions $V_{dm4}(\phi)$ is calculated as:

$$V_{dm4}(\phi) = \sqrt{\frac{2gE_{dm4}(\phi)}{W}} \tag{5}$$

where g is gravitational acceleration and W is the total weight of the building. The angle ϕ_c at which $V_{dm4}(\phi)$ is maximized generally corresponds to the direction of collapse.

Fig. 4 shows the $V_{dm4}(\phi_c)$ curves obtained by inputting half-cycle sine waves with polar coordinates. The $V_{dm4}(\phi_c)$ curves represent the seismic energy capacity of a frame. For the frames with $t_c = 9$ and 12 mm, most of the plastic hinges formed at the column ends due to the story-collapse mechanism, and thus the energy absorption of the columns dominates. The curve of columns under biaxial bending becomes almost circular. The curves are thus almost circular arcs. For the frames with $t_c = 16$ mm, most of the plastic hinges formed at the beam ends due to the total-collapse mechanism, and thus the energy absorption of the beam dominates. The curve of beams becomes almost rectangular because beams in orthogonal frames absorb energy independently. Therefore, the curves are almost rectangular.

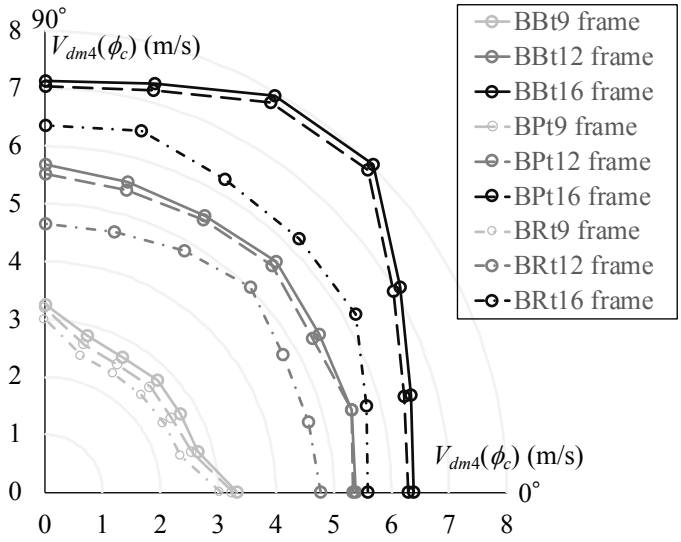

Fig. 4 – Energy capacity curves obtained for half-cycle sine waves

Fig. 5 shows the $V_{dm4}(\phi_c)$ curves obtained for half-cycle sine waves and seismic waves with polar coordinates. The hyphenated numbers in Fig. 4 indicate the ranges of fully collapsed stories. For the frames with t_c = 9 and 12 mm, the $V_{dm4}(\phi_c)$ curves obtained for seismic waves are in good agreement with the energy capacity curves obtained for half-cycle sine waves. For the frames with t_c = 16 mm, the $V_{dm4}(\phi_c)$ curves obtained for seismic waves are larger than the energy capacity curves obtained for half-cycle sine waves. Because the frame has high plastic deformation capacity, the number of plastic deformations during an earthquake is large. The frame thus absorbs more energy when subjected to an earthquake than when subjected to half-cycle sine waves. In other cases, the number of collapsed stories was different between seismic waves and half-cycle sine waves. The factors responsible for this difference will be examined in the future. Nevertheless, the $V_{dm4}(\phi_c)$ under an earthquake can be evaluated on the safe side with energy capacity curves obtained for half-cycle sine waves.

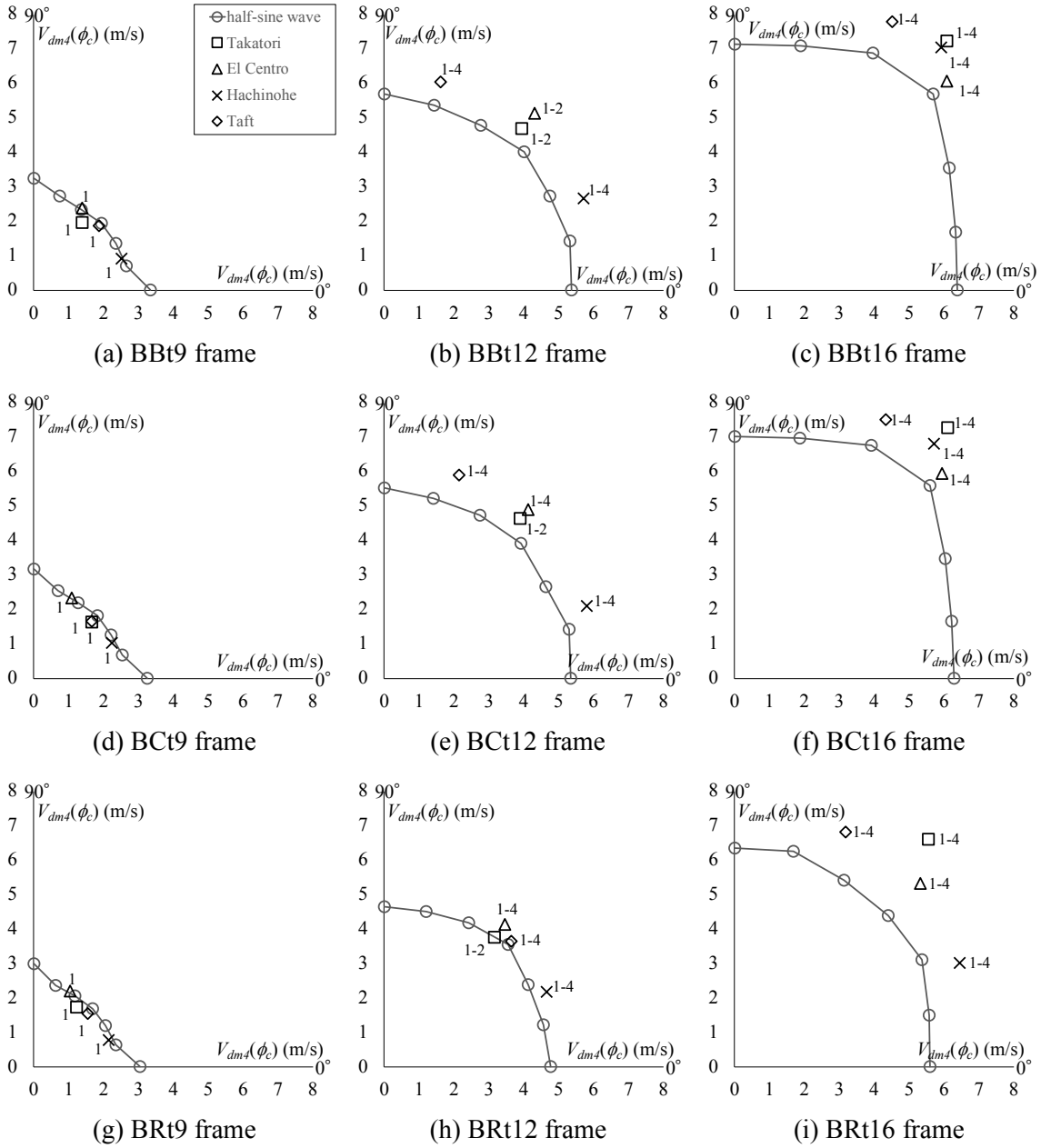

(a) BBt9 frame (b) BBt12 frame (c) BBt16 frame

(d) BCt9 frame (e) BCt12 frame (f) BCt16 frame

(g) BRt9 frame (h) BRt12 frame (i) BRt16 frame

Fig. 5 – $V_{dm4}(\varphi_c)$ obtained for half-cycle sine waves and seismic waves

4. Conclusion

This study conducted seismic response analyses using three-dimensional frames with the column design specifications used as parameters. The collapse behavior and the energy absorption performance of frames with different specifications were considered. The following results were obtained.

(1) In the three-dimensional analysis, it was confirmed that the apparent column-to-beam strength ratio, considering the biaxial bending of the column, affects the number of collapsed stories.
(2) The values of $V_{dm4}(\phi_c)$ in the diagonal direction tended to be higher than those in the straight diagonal direction for frames that exhibited the total-collapse mechanism. The opposite trend was observed for frames that exhibited the story-collapse mechanism.
(3) The $V_{dm4}(\phi_c)$ for seismic wave input can be evaluated on the safe side using half-cycle sine waves.

5. References

[1] Yamada S, Suita K, Tada M, Kasai K, Matsuoka Y, Shimada Y (2008): Collapse Experiment on 4-Story Steel Moment Frame: Part 1 Outline of Test Results. *14th World Conference on Earthquake Engineering*, Beijing, China.

[2] Suita K, Yamada S, Tada M, Kasai K, Matsuoka Y, Shimada Y (2008): Collapse Experiment on 4-Story Steel Moment Frame: Part 2 Detail of Collapse Behavior. *14th World Conference on Earthquake Engineering*, Beijing, China.

[3] Tada M, Horimoto A, Mitani A, Mukaide S, Kasai K, Suita K, Yamada S (2010): Numerical Simulation of Collapse using Collaborative Structural Analysis System. *7th International Conference on Urban Earthquake Engineering and 5th International Conference on Earthquake Engineering*, 879-885.

[4] Matsukawa D, Mukaide S (2019): Modeling of columns in Steel Moment-Resisting Frames During collapse under Severe Earthquake. *Proceedings of 12th Pacific Structural Steel Conference*, Tokyo, Japan.

[5] Yamada A, Ishida T, Shimada Y (2012): Hysteresis Model of RHS Columns in the Deteriorating Range Governed by Local Buckling. *Journal of Structural and Construction Engineering*, AIJ, No.674, 627-636 (in Japanese).

[6] Yamada A, Akiyama H, Kuwamura H (1993): Post-Buckling and Deteriorating Behavior of Box-Section Steel Members. *Journal of Structural and Construction Engineering*, AIJ, No.444, 135-143 (in Japanese).

[7] Kato B (1987): Deformation capacities of Tubular Steel Members Governed by Local Buckling. *Journal of Structural and Construction Engineering*, AIJ, No.378, 27-36 (in Japanese).

[8] Meng L, Ohi K, Takanashi K (1992): A Simplified Model of Steel Structural Members with Strength Deterioration Used for Earthquake Response Analysis. *Journal of Structural and Construction Engineering*, AIJ, No.437, 115-124 (in Japanese).

[9] Murakami Y, Mukaide S, Tada M (2013): Comparison of the Properties to be Collapse for the Three-Dimensional Moment Resistant Frame against a Variety of Ground Motion, *Summaries of Technical Papers of Annual Meeting*, AIJ, C-1,1027-1028 (in Japanese).

[10] Morimae N, Mukaide S, Tada M (2014): Energy absorbing Characteristics of the Collapsing Three-Dimensional Moment Resistant Frame against a variety of Ground Motion. *Summaries of Technical Papers of Annual Meeting*, AIJ, C-1, 1039-1040 (in Japanese).

[11] Mukaide S, Tada M (2015): Numerical Analysis of collapsing Behavior for Steel Moment frames, *Proceedings of the IABSE Conference*, Nara, Japan

